A comparison of potential healing agents for vascular-based self-healing concrete

Yasmina Shields[1], *Vanessa* Cappellesso[1,2], *Tim* Van Mullem[1], *Nele* De Belie[1], and *Kim* Van Tittelboom[1]

[1]Magnel-Vandepitte Laboratory, Department of Structural Engineering and Building Materials, Faculty of Engineering and Architecture, Ghent University, Technologiepark Zwijnaarde 60, B-9052 Ghent, Belgium

[2]KU Leuven, Department of Civil Engineering, Materials and Constructions, Ghent Technology Campus, Gebroeders De Smetstraat 1, 9000 Ghent, Belgium

Abstract. Vascular self-healing concrete is an innovative technology that can potentially improve the durability and longevity of concrete structures. However, limited research is available concerning this type of self-healing compared to intrinsic or capsule-based healing. As the rheology and curing properties of a healing agent can dictate the optimal design configuration of a vascular network, a series of testing procedures for evaluating healing agents is further explored. In this study, the suitability of various commercially available healing agents is considered using a vascular network system in mechanical loading and water absorption test set-ups. In this particular configuration, high sealing efficiencies were obtained for most of the healing agents used, and the polyurethanes and epoxy resin that were studied showed high load regain values. This work provides a testing methodology to select a healing agent in terms of its mechanical load regain, sealing efficiency, rheology, and curing properties, and can be used to determine a suitable healing agent for vascular healing applications.

1 Introduction

Vascular self-healing refers to the ability of a material to repair itself in a similar way to how the human body's vascular system heals wounds [1]. This typically employs internal channels or conduits that transport healing agents to damaged areas of the structure on an as-needed basis, rather than waiting for repairs to be made by human intervention. This type of self-healing technology is still in the development phase, but has the potential to greatly improve the durability and longevity of concrete structures.

An epoxy resin, two polyurethanes and two water repellent agents are investigated in this work. Previous studies in self-healing materials have shown the effectiveness of epoxy resin as a healing agent given its chemical resistance and interesting mechanical properties [2–4]. Foaming polyurethane has also been used in vascular self-healing applications [5–7], with potential for enhanced healing due to its expansive foaming reaction with moisture. Water repellent agents are an additional promising healing agent for vascular networks as they have a relatively lower viscosity (<10 mPa.s), making them more suitable for pumping across a large network as well as through smaller crack widths [8–9].

2 Materials and methods

2.1 Healing agents

An overview of the selected healing agents and their key characteristics are summarized in Table 1. Each healing agent has a different hardening mechanism. The epoxy resin used in this study is a two-component resin, which hardens upon reaction of the two components. Both types of polyurethane react with moisture present in the air or at the concrete surface, and the water repellents react with hydrated cement to form a hydrophobic silicon resin along the walls of the concrete crack.

Table 1. Healing agent characteristics.

Code Name	Type of polymer	Curing time @ 20°C	Viscosity @ 20°C (mPa.s)
ER	Epoxy	30 min	160
PU_1	Polyurethane	24 hrs	390
PU_2	Polyurethane	1-5 min	4200
WRA_1	Silane	4 hrs	2.6
WRA_2	Silane	24 hrs	7

2.2 Concrete composition

The concrete used in this study consisted of: 341 kg/m^3 CEM I 52.5 N, 672 kg/m^3 sand (0-4 mm), 766 kg/m^3 gravel (2-8 mm), 182 kg/m^3 limestone filler, and 8.98 kg/m^3 superplasticizer (Master Glenium 27 concentration of 20%, BASF, Waterloo, Belgium). After the dry components were mixed for one minute, water was added and mixing continued for an additional three minutes. Superplasticizer was added 30 seconds after water was mixed in. The concrete was added into molds with dimensions of 60 x 60 x 220 mm^3 in two layers, and was vibrated at a low frequency for no more than 20 seconds. After casting, the samples were placed in a curing room with a temperature of 20°C and a relative humidity of >95%. The specimens were demolded one day after casting, and were immediately placed back in the curing environment for two weeks until testing.

2.3 Vascularized prisms

The vascular network included a series of three 150 mm long glass tubes which were sanded to promote bonding to the surrounding matrix. Two 2-mm diameter copper-coated sanded steel wires to prevent the prisms from completely breaking in two parts during mechanical loading. The reinforcement was located 12 mm from the bottom of the prism and 10 mm from the side of the prism. The glass tubes had an outer diameter of 3.8 mm and a wall thickness of 0.8 mm; two tubes were placed in the molds directly above the reinforcement, and the third was placed centered and in line with the other glass tubes (Figure 1). As a brittle material, the glass networks would break upon loading of the concrete prism, thereby later allowing a healing agent to flow out of the network and into the crack. The prisms were notched to a depth of 4 mm using a mechanical saw at the bottom midspan to promote crack formation in the center of the prism.

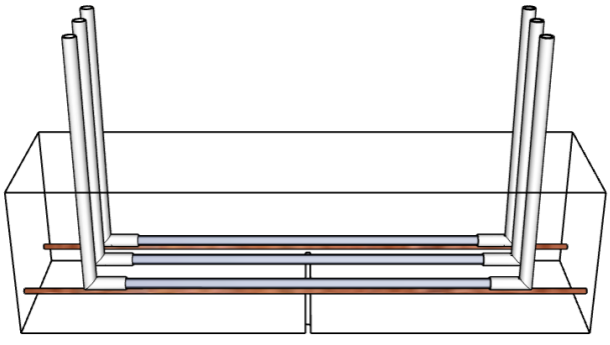

Figure 1. Vascular network schematic.

Three repetitions for each healing agent were produced, as well as three uncracked (UNCR) and three cracked (REF CR) reference samples (all containing networks that would not be filled with a healing agent).

2.4 Preliminary characterization of water repellent agents

Sessile drop tests were performed to characterize the hydrophobic behavior that results in the potential sealing performance of the two water repellent agents. Concrete surfaces of 60 mm x 60 mm using the same mix design as mentioned previously were prepared by manually brushing a layer of the water repellent agent. The water repellent agents were applied to the samples in two coats of 0.5 mL, one immediately following the other, and left in a climate-controlled room at 20°C and 60 % of relative humidity for three days.

The sessile drop test consisted of applying a drop of distilled water over the (un)treated sample surfaces with a maximum velocity rate of 904 µm/min and measuring the contact angle formed at the interface of the drop and the surface using a high-speed camera.

2.5 Healing evaluation

In order to generate a crack, the prisms were loaded in 3-point bending with a span of 190 mm using a universal load frame (Instron Model 5982). Cracking was controlled using crack mouth opening displacement (CMOD) gauge at the midspan of the prism with a rate of 0.7 µm/s. The test concluded once a CMOD reading of 0.4 mm was achieved, so that the relaxed crack width would reach approximately 0.3 mm after unloading of the sample.

Self-sealing efficiency was evaluated via a series of two capillary water absorption tests: one before and one after the supply of the healing agent. The purpose of this is to allow an evaluation of the same crack before and after healing, rather than relying on an average efficiency value over multiple samples. After crack formation, all specimens were placed in an oven at 40 ± 5 °C for a period of 5 days. Two coatings of an epoxy resin sealer were then applied to the samples with a brush, allowing for a 14 mm exposed strip centered on the crack along the bottom and sides of the specimen, based on [10]. Once the coating was applied and cured, the samples were placed back in the oven at 40 ± 5 °C for an additional 5 days. The capillary water absorption test then proceeded by placing the samples in a box containing water so that the specimens were immersed in water 3 ± 1 mm above the top of the notch. The specimens were weighed after 10 min, 20 min, 30 min, 1 h, 1 h 30 min, 2 h, 3 h, 4 h, 6 h, 8 h, and 24 h. The samples were dried for a period of 10 days after the first water absorption test, then healed with different healing agents. The samples were pumped with the healing agents using a peristaltic pump until a pressure of 1.5 bar was achieved, and allowed 24 hours for curing before the second water absorption test. The sealing efficiency could then be calculated as follows:

$$SE = \frac{\frac{SC_{Unhealed,1st\ test}}{SC_{UNCR,1st\ test}} - \frac{SC_{Healed,2nd\ test}}{SC_{UNCR,2nd\ test}}}{\frac{SC_{Unhealed,1st\ test}}{SC_{UNCR,1st\ test}} - 1} \ x\ 100\% \quad (1)$$

where $SC_{Unhealed,\ 1st\ test}$ corresponds to the sorption coefficient (SC, obtained by the linear slope line for the

cumulative mass gain over the square root of time graphs, in g/√h) for the first water absorption test of the unhealed series, $SC_{Healed,\ 2nd\ test}$ corresponds to the SC of the same samples after they are healed in the second test, and $SC_{UNCR,\ 1st\ test}$ corresponds to the SC of the uncracked series from the first test.

Three days after the second capillary water absorption test, the samples were reloaded using the same criteria used in the first loading test, in order to obtain an evaluation on regain in mechanical strength. Afterwards, samples were broken along the crack face to visually inspect the healing agent spread. The mechanical load recovery was evaluated by a load regain index (LRI) defined by [11-12] as:

$$LRI\ (\%) = \frac{P_r - P_u}{P_p - P_u}\ x\ 100\% \qquad (2)$$

where P_r (kN) is the maximum load obtained during reloading, P_p (kN) is the peak load during the first loading, and P_u (kN) is the residual load obtained at the moment of unloading during the first loading cycle. If no clear peak was achieved upon reloading, P_r was assumed to be the point along the curve where the slope starts to change.

3 Results and discussion

3.1 Capillary water absorption and sessile drop tests

The cumulative water absorption over the square root of time is plotted for each series of specimens in Figure 2. All of the healing agents attained high amounts of sealing, as they absorbed significantly less water than both the reference cracked and uncracked samples, which is possible due to the fact that they became very well sealed by the healing agents.

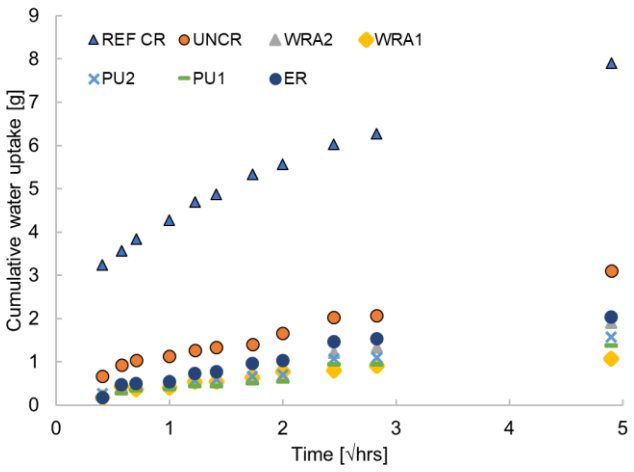

Figure 2. Mean values for cumulative water absorption over time for the second water absorption tests (after samples have been healed). Error bars are omitted for clarity.

Figure 3 reports the sealing efficiencies as calculated by Equation 1. Of the studied healing agents, WRA_1 performed the best with a sealing efficiency of 178%, and all other healing agents reported sealing efficiencies between 122-145%, further quantifying the well-sealed quality that the healing agents impart on the prisms.

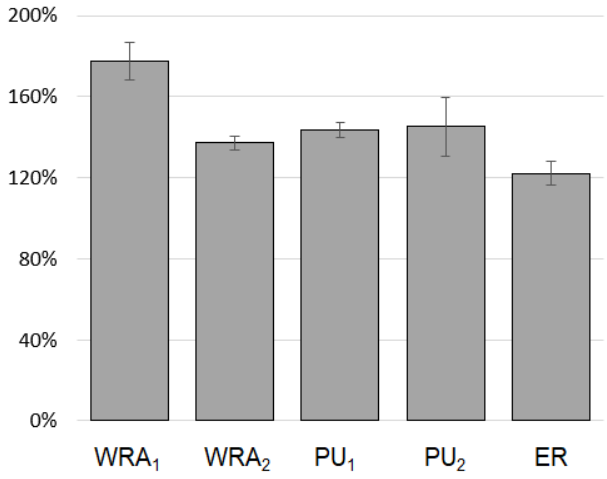

Figure 3. Sealing efficiencies; error bars indicate the standard deviation of three samples.

The relative increase in healing efficiency between WRA_1 and WRA_2 can be attributed to the results obtained by the sessile drop tests performed on treated concrete surfaces (Figure 4). The surface treated with WRA_2 measured an average contact angle of 74.4°, while the surface treated with WRA_1 obtained a larger angle of 87.9°, indicating a higher water repellence (a reference untreated series obtained a contact angle of 30.3°).

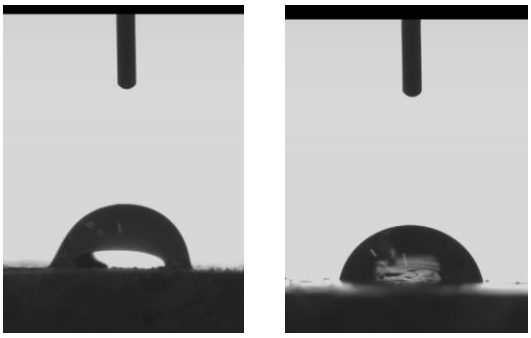

Figure 4. Images from the sessile drop test from a) WRA_1 and b) WRA_2.

3.2 Mechanical load regain

Load regain index calculations are summarized in Figure 5. Significant load regains above 150% are noted for the epoxy resin and both polyurethanes. In addition, some unexpected amount of load regain was also noticed for WRA_2.

Figure 5. Load regain index (LRI) of each series. Error bars indicate standard deviation of three samples.

Although all samples which were healed with an adhesive (PU_1, PU_2 and ER) achieved high load regain index (LRI) values (>150%), there is a notable difference between each series and thus each healing agent can be easily ranked in order of increasing efficiency. Another aspect to consider is the flexibility of the healing agents. While the series with the best load regain values, PU_2 and ER, achieved LRI values of 195% and 257%, respectively, they showed a brittle response and some of the samples produced a new crack upon reloading. The flexibility of a healing agent can therefore be an additional criterion for selecting a healing agent.

3.3 Healing agent coverage by visual inspection

Once the samples were reloaded, they were broken along the crack wall in order to visually inspect spread of the healing agent throughout the surface of one of the halves. The epoxy resin samples were unable to be opened along the crack face since a new crack had reformed alongside the already healed crack from the first loading. In Figure 6, the areas marked in red indicate the areas where the healing agents PU and WRA had reached throughout the crack surface. It is noted that the WRA_1 series had agent absorbed all the way up to the uppermost tip of the crack and was capable of covering the entirety of the cross-section, achieving an average coverage of 100% of the surface area. PU_1 and PU_2 behaved similarly (despite the large difference in viscosity), with 87% and 84% coverage. This can be attributed to the fact that the vascular network system was pressurized with a high pressure relative to the network dimensions. WRA_2 had the least amount of coverage with 66%; however, this did not hinder its high sealing efficiency reported in Figure 3. As can be seen by the representative specimen in Figure 6, WRA_2 was able to cover the bottom half of the crack surface, thereby providing an uninterrupted protection against water absorption.

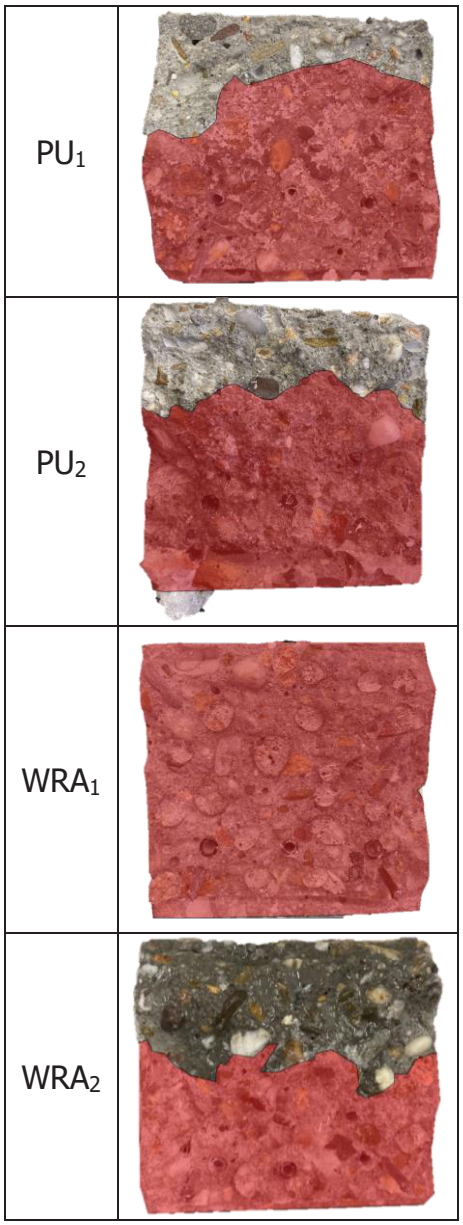

Figure 6. Highlighted cross-sections of healing agent distribution throughout crack for representative samples in each series.

4 Conclusion

This work provides a basis to evaluate the durability and mechanical regain performance of various commercially available healing agents using a linear glass vascular network scheme. All healing agents achieved sealing efficiencies above 100%. Additional characterization tests were carried out on the water repellent agents, where a higher measured contact angle for WRA_1 accounts for its superior performance. Surprisingly, some amount of load regain was seen for WRA_2, and all other healing agents showed good mechanical regain performance in this particular testing set-up. This series of tests and prism set-up can be used for future standardization tests to help evaluate potential healing agents given a certain application.

This project received funding from the European Union's Horizon 2020 research and innovation program under the Marie Sklodowska-Curie grant agreement No 860006.

References

[1] Y. Shields, N. De Belie, A. Jefferson, and K. Van Tittelboom, "A review of vascular networks for self-healing applications," *Smart Mater. Struct.*, vol. 30, no. 6, 2021, doi: 10.1088/1361-665X/abf41d.

[2] K. Van Tittelboom and N. De Belie, *Self-healing in cementitious materials-a review*, vol. 6, no. 6. 2013.

[3] C. J. Hansen, W. Wu, K. S. Toohey, N. R. Sottos, S. R. White, and J. A. Lewis, "Self-healing materials with interpenetrating microvascular networks," *Adv. Mater.*, vol. 21, no. 41, pp. 4143–4147, Nov. 2009, doi: 10.1002/adma.200900588.

[4] A. R. Hamilton, N. R. Sottos, and S. R. White, "Pressurized vascular systems for self-healing materials," *J. R. Soc. Interface*, vol. 9, no. 70, pp. 1020–1028, 2012, doi: 10.1098/rsif.2011.0508.

[5] P. Minnebo, G. Thierens, G. De Valck, K. Van Tittelboom, and N. De Belie, "A Novel Design of Autonomously Healed Concrete :," *Materials (Basel).*, pp. 1–23, 2017, doi: 10.3390/ma10010049.

[6] E. Tsangouri, C. Van Loo, Y. Shields, N. De Belie, K. Van Tittelboom, and D. G. Aggelis, "Reservoir-Vascular Tubes Network for Self-Healing Concrete: Performance Analysis by Acoustic Emission, Digital Image Correlation and Ultrasound Velocity," *Appl. Sci.*, vol. 12, no. 10, 2022, doi: 10.3390/app12104821.

[7] B. Van Belleghem, K. Van Tittelboom, and N. De Belie, "Efficiency of self-healing cementitious materials with encapsulated polyurethane to reduce water ingress through cracks," *Mater. Constr.*, 2018, doi: 10.3989/mc.2018.05917.

[8] K. Van Tittelboom, C. De Maesschalck, B. Van Belleghem, P. den Heede, S. Kessler, and N. De Belie, "Self-healing of concrete cracks by the release of embedded water repellent agents and corrosion inhibitors to reduce the risk for reinforcement corrosion," *14th Int. Conf. Durab. Build. Mater. Components (XIV DBMC 2017)*, vol. 107, no. Ci, pp. 1–10, 2017.

[9] J. G. Dai, Y. Akira, F. H. Wittmann, H. Yokota, and P. Zhang, "Water repellent surface impregnation for extension of service life of reinforced concrete structures in marine environments: The role of cracks," *Cem. Concr. Compos.*, vol. 32, no. 2, pp. 101–109, 2010, doi: 10.1016/j.cemconcomp.2009.11.001.

[10] T. Van Mullem *et al.*, "Addressing the need for standardization of test methods for self-healing concrete: an inter-laboratory study on concrete with macrocapsules," *Sci. Technol. Adv. Mater.*, 2020, doi: 10.1080/14686996.2020.1814117.

[11] G. Anglani, P. Antonaci, S. Carillo Gonzales, G. Paganelli, and J. Tulliani, "3D printed capsules for self-healing concrete applications," no. June, 2019, doi: 10.21012/fc10.235356.

[12] A. Formia *et al.*, "Experimental analysis of self-healing cement-based materials incorporating extruded cementitious hollow tubes," *J. Intell. Mater. Syst. Struct.*, vol. 27, no. 19, pp. 2633–2652, 2016, doi: 10.1177/1045389X16635847.